

# Chemically Modified Nanofoci Unifying Plasmonics and Catalysis

Yueliang Wang,<sup>†</sup> Lingling Fang,<sup>†</sup> Ming Gong,<sup>‡</sup> and Zhaoxiang Deng<sup>\*,†</sup>

<sup>†</sup>CAS Key Laboratory of Soft Matter Chemistry, Hefei National Research Center for Physical Sciences at the Microscale, Department of Chemistry, University of Science and Technology of China, Hefei, Anhui 230026, China

<sup>‡</sup>Engineering and Materials Science Experiment Center, University of Science and Technology of China, Hefei, Anhui 230027, China

Email: zhxdeng@ustc.edu.cn

## Experimental Details

### Chemicals

Chloroauric acid tetrahydrate ( $\text{HAuCl}_4 \cdot 4\text{H}_2\text{O}$ ), hexachloroplatinic acid hexahydrate ( $\text{H}_2\text{PtCl}_6 \cdot 6\text{H}_2\text{O}$ ), hydrogen peroxide, hydrochloric acid, Polyvinylpyrrolidone (K30), and sodium borohydride ( $\text{NaBH}_4$ ) were obtained from Sinopharm Chemical Reagent Co., Ltd. (Shanghai, China). Fish sperm DNA (FSDNA) and sodium citrate tribasic dihydrate were bought from Sigma. Bis (p-sulfonatophenyl) phenylphosphine dihydrate dipotassium salt (BSPP) and sodium tetrachloropalladate trihydrate ( $\text{Na}_2\text{PdCl}_4 \cdot 3\text{H}_2\text{O}$ ) were obtained from Strem Chemicals (Newburyport, MA, USA). 4-nitrophenol (4-NTP) and 4-aminothiophenol (4-ATP) were purchased from J&K Chemicals (Beijing, China).  $\text{AgNO}_3$  was a product from Bio Basic Inc. (BBI, Canada). All reagents were used as received without further purifications.

### DNA sequences

DNA oligonucleotides were custom-synthesized by Sangon Bioengineering Technology and Services Co., Ltd. (Shanghai, China) and purified by PAGE (unmodified DNA) or HPLC (thiolated DNA). All DNA oligos were subject to a molecular weight verification by MALDI-TOF mass spectroscopy. Following are the sequences (5'-3') of the DNA oligonucleotides used in this work (*Note*: underlined sequences in sDNA and sDNAc are complementary to each other; sDNA and sDNAc were modified versions of a sequence used in: *Nano Letters* **2001**, 1, 32)):

#### sDNA (89 bases):

HS-5'GCAGTAACGCTATGTGACCGAGAAGGATTCGCATTTGTAGTCTTGAGCCCGCACGAAACCTG  
GACACCCCTAAGCAACTCCGTATCAGA3'

#### sDNAc (89 bases):

HS-5'GCAGTAACGCTATGTGACCGAGAAGGATTCGCATTTGTATCTGATACGGAGTTGCTTAGGGGT  
GTCCAGGTTTCGTGCGGGCTCAAGAC3'

**AuNPs:** AuNPs with different diameters of 23, 30, and 43 nm were synthesized through a seeded-growth described in a previous publication. [N. G. Bastús, J. Comenge, V. Puntes, *Langmuir* 2011, 27,

11098-11105]. The as-obtained citrate-capped nanoparticles were incubated overnight with Bis (*p*-sulfonatophenyl)phenylphosphine dihydrate dipotassium salt (BSPP) (0.5 mg/mL for 23 and 30 nm AuNPs, 1 mg/mL for 43 nm AuNPs) at room temperature to accomplish a ligand exchange. The BSPP-decorated AuNPs were collected by centrifugation and redispersed in 0.5 mL of deionized H<sub>2</sub>O.

**AIS-assembled AuNP dimers:** The BSPP-capped AuNPs were added to a 0.5×TBE (pH 8.0; 44.5 mM Tris, 1 mM EDTA, 44.5 mM boric acid) buffer supplemented with 11 mM AgNO<sub>3</sub> and 2 μg/μL FSDNA at room temperature for 1 min. The resulting discrete AuNP clusters were further isolated by agarose gel electrophoresis to obtain dimeric assemblies in purified form.

**g-dimers and s-dimers:** A 20 μL solution of 38.8 mM sodium citrate and different volumes of 1 mM HAuCl<sub>4</sub> or AgNO<sub>3</sub> were added to 1 mL boiling water containing 0.1 nM AuNP dimers. The solution was kept boiling in a 125°C oil bath, and maintained under this condition for 20 min to obtain gold and silver modified dimers with different junction widths.

**Pt-s-dimers:** To 4 mL of boiling water containing 0.1 nM s-dimers (made from 35 nm AuNPs and pre-incubated with 0.1% PVP) was added 20 μL of a 20 mM H<sub>2</sub>PtCl<sub>6</sub> solution. The resulting mixture was stirred for 2 min in a 115°C oil bath, followed by an addition of 20 μL of an aqueous PVP solution (20 %). After a 20 min incubation with PVP, the solution was centrifuged at 2390 g to precipitate the Pt-s-dimers, which were then redispersed in water for further use.

**Pd-s-dimers:** An 80 μL solution containing 2.5 mM Na<sub>2</sub>PdCl<sub>4</sub> was added to a 4mL solution containing 0.1 nM s-dimers (made from 35 nm AuNPs and pre-incubated with 0.1% PVP). The solution was stirred for 10 min in an ice-water bath to obtain Pd-s-dimers. Afterwards, 20 μL of a PVP aqueous solution (20 %) was introduced for an extra protection of the products. After a 20 min incubation with PVP, the solution was subjected to a centrifugation at 2390 g. The precipitated Pd-s-dimers were redispersed in water for further use.

**DNA-monofunctionalized 5 nm AuNPs:** BSPP-capped 5 nm AuNPs synthesized by a sodium citrate/tannic acid method (*Eur. J. Cell Biol.* 1985, 38, 87-93) were combined with 5'-thiolated DNA stands at a molar ratio of 1:0.6 (AuNP:DNA) in 0.5×TBE (pH 8.0) supplemented with 100 mM NaCl. After a 2h incubation at 20°C, the mixture was purified by 3% agarose gel electrophoresis to obtain monovalent DNA-AuNP conjugates.

**DNA multifunctionalized g-dimers:** G-dimers made from 23 nm AuNPs were combined with 5'-thiolated DNA stands at a molar ratio of 1:500 in 250 μL of a 0.5×TBE (pH 8.0) buffer. 3.75 μL of NaNO<sub>3</sub> (1 M) was added to this solution every 3 hours for 23 times. The final solution was centrifuged at 6120 g with the solid pallet redispersed in the 0.5×TBE buffer. This process was repeated 3 times to remove unbound DNA stands.

**DNA-directed core-satellite assemblies between g-dimers and AuNPs:** DNA-multifunctionalized g-dimers and DNA-monofunctionalized 5 nm AuNPs bearing complementary DNA sequences were combined at a molar ratio of 1:500 in 0.5×TBE containing 150 mM NaNO<sub>3</sub>. The mixture was kept at 37°C for 24 h to form core-satellite assemblies via DNA hybridization. 0.6% agarose gel electrophoresis was employed to isolate the products.

**H<sub>2</sub>O<sub>2</sub> etching of s-dimers:** Different amounts of H<sub>2</sub>O<sub>2</sub> were added to a 30 μL solution of 1 nM 30 nm s-dimer buffered with 0.1×TBE (pH 8.0) for a 20 s etching.

**4-NTP decorated CMNFs:** A 1 μL aqueous droplet containing appropriate amounts of 4-NTP was added separately to 100 μL solutions of 0.2 nM AIS-assembled AuNP dimers (35 nm) and CMNF structures (s-dimers, Pt-s-dimers, Pd-s-dimers) followed by a 30 min adsorption. Free unbound 4-NTP in excess was removed by centrifugation at 2390 g with the precipitates being redispersed in deionized water.

**Catalytic NaBH<sub>4</sub> reduction of 4-NTP:** 1 μL of 50 mM NaBH<sub>4</sub> was combined with the 4-NTP-decorated Au nanodimers and CMNFs (0.2 nM) to initiate a hydrogenation of 4-NTP to form 4-ATP.

**TEM characterizations:** TEM imaging was conducted on a Hitachi HT7700 transmission electron microscope operated at an electron acceleration voltage of 100 kV. An aqueous sample droplet was pipetted on a carbon-coated copper grid, followed by a removal of the liquid after a 10 min deposition.

**Spectroscopic characterizations:** UV-vis extinction spectra were recorded on a Hitachi U-2910 spectrophotometer. Raman spectra were measured for liquid samples in a low-volume quartz cuvette at room temperature with a portable Raman spectrometer (Ocean Optics) equipped with a Maya 2000 CCD detector and a 671 nm laser.

**Energy dispersive X-ray spectroscopic (EDX) analysis:** EDX element analysis of a sample was conducted on a JEM-2100F field emission transmission electron microscope operated at an electron acceleration voltage of 200 kV.

## Supporting figures

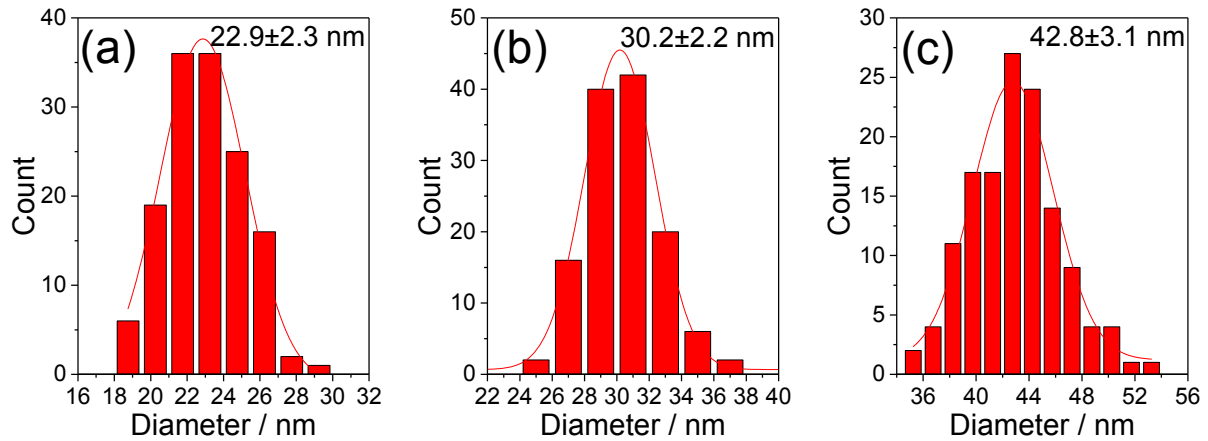


**Figure S1.** Statistical diameter distributions of as-synthesized 23, 30, and 43 nm AuNPs used throughout our experiments.

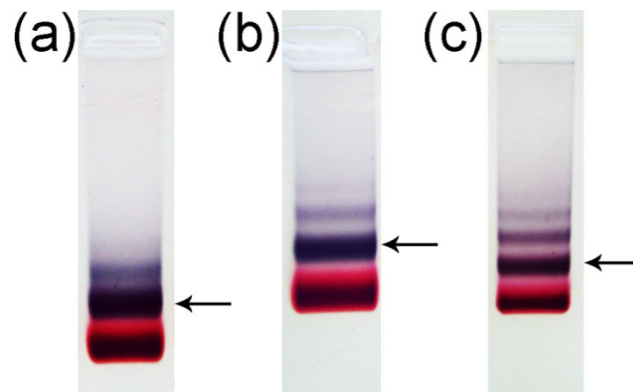


**Figure S2.** Agarose gel electrophoretic purifications of  $\text{Ag}^+$ -soldered Au nanoparticle dimers with different diameters of 23 nm (a), 30 nm (b), and 43 nm (c). The bands marked by arrows are dimeric products which can be eluted from the gels.

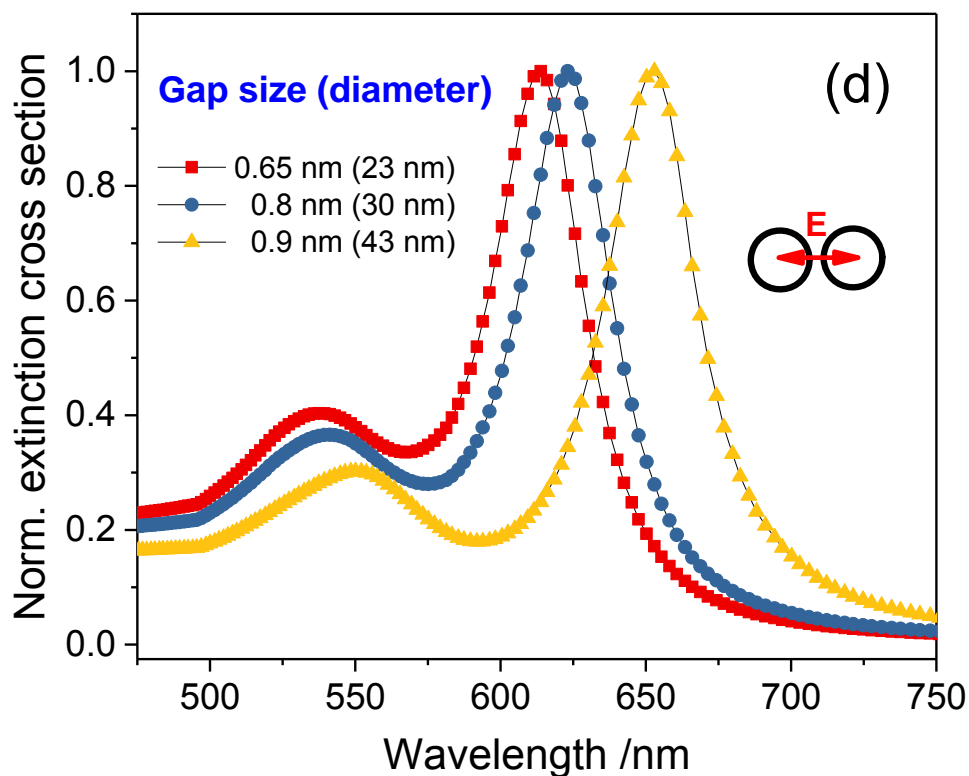
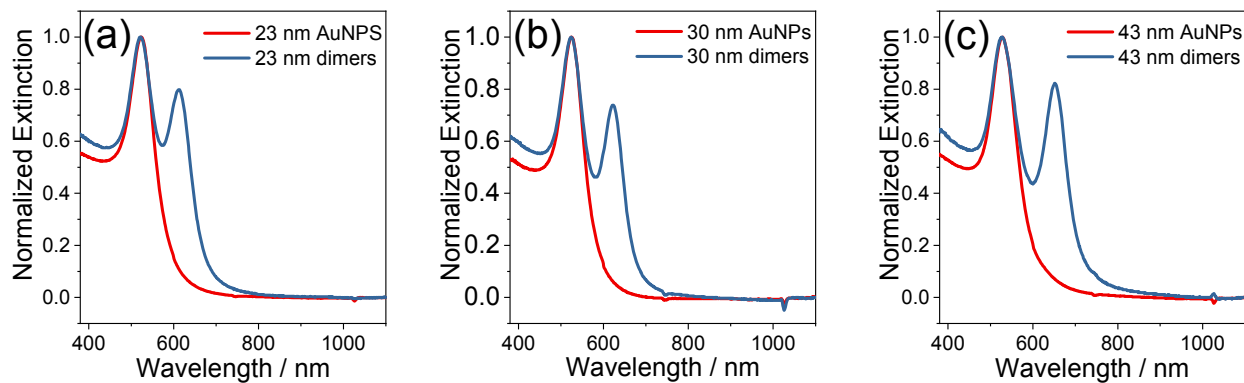


**Figure S3.** Normalized extinction spectra of (a) 23, (b) 30 and (c) 43 nm gold nanoparticles along with their dimers assembled by  $\text{Ag}^+$  soldering. (d) Simulations of the coupling-induced longitudinal plasmon (BDP) resonances of the dimers indicated gap separations of (a) 0.65 nm, (b) 0.8 nm, and (c) 0.9 nm for the 23-43 nm dimers, respectively. Light polarization was along the dimer axis. The simulations were carried out by a MESME algorithm developed by Prof. García de Abajo (F. J. Garcia de Abajo, Phys. Rev. Lett. 1999, 82, 2776; F. J. Garcia de Abajo, Phys. Rev. B 1999, 60, 6086).

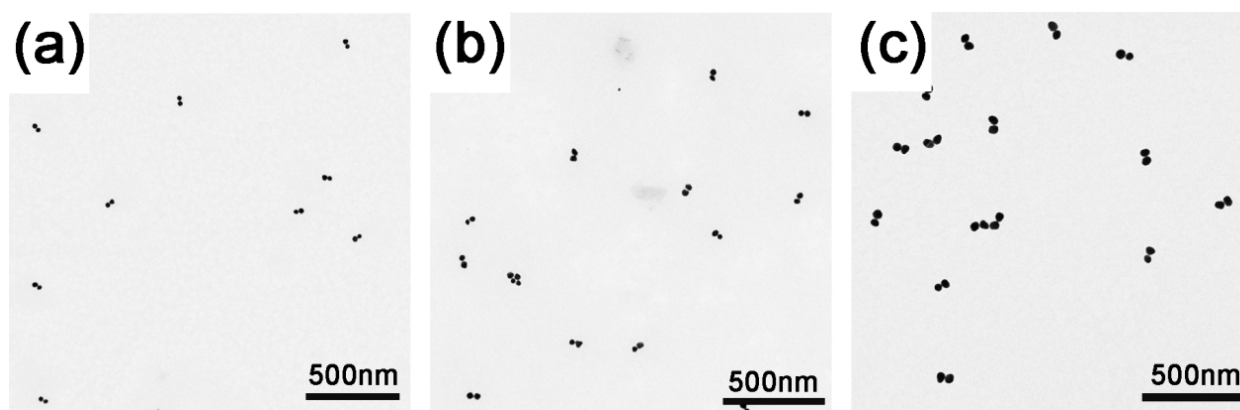


**Figure S4.** TEM images of gel-isolated dimeric clusters of AuNPs with different diameters of 23 nm (a), 30 nm (b), and 43 nm (c).

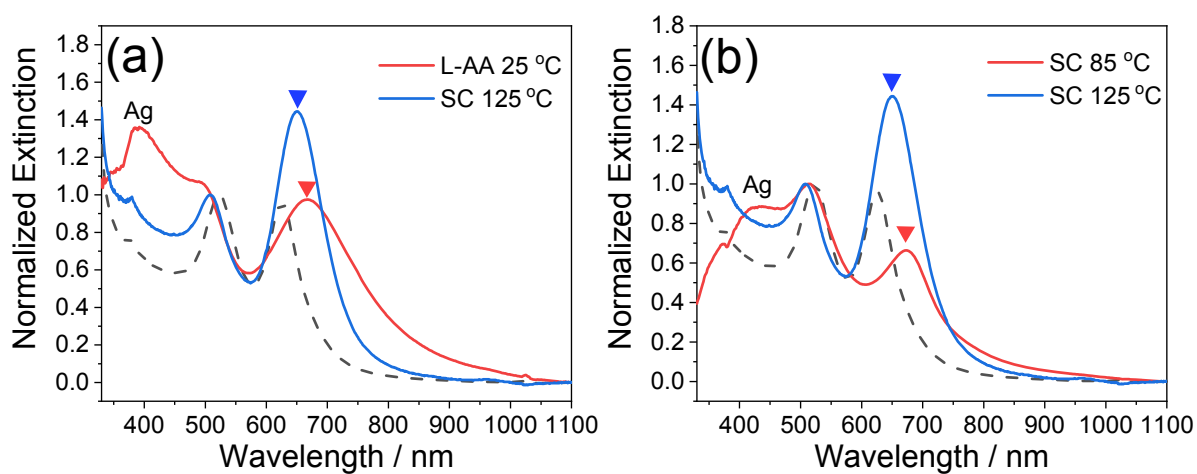
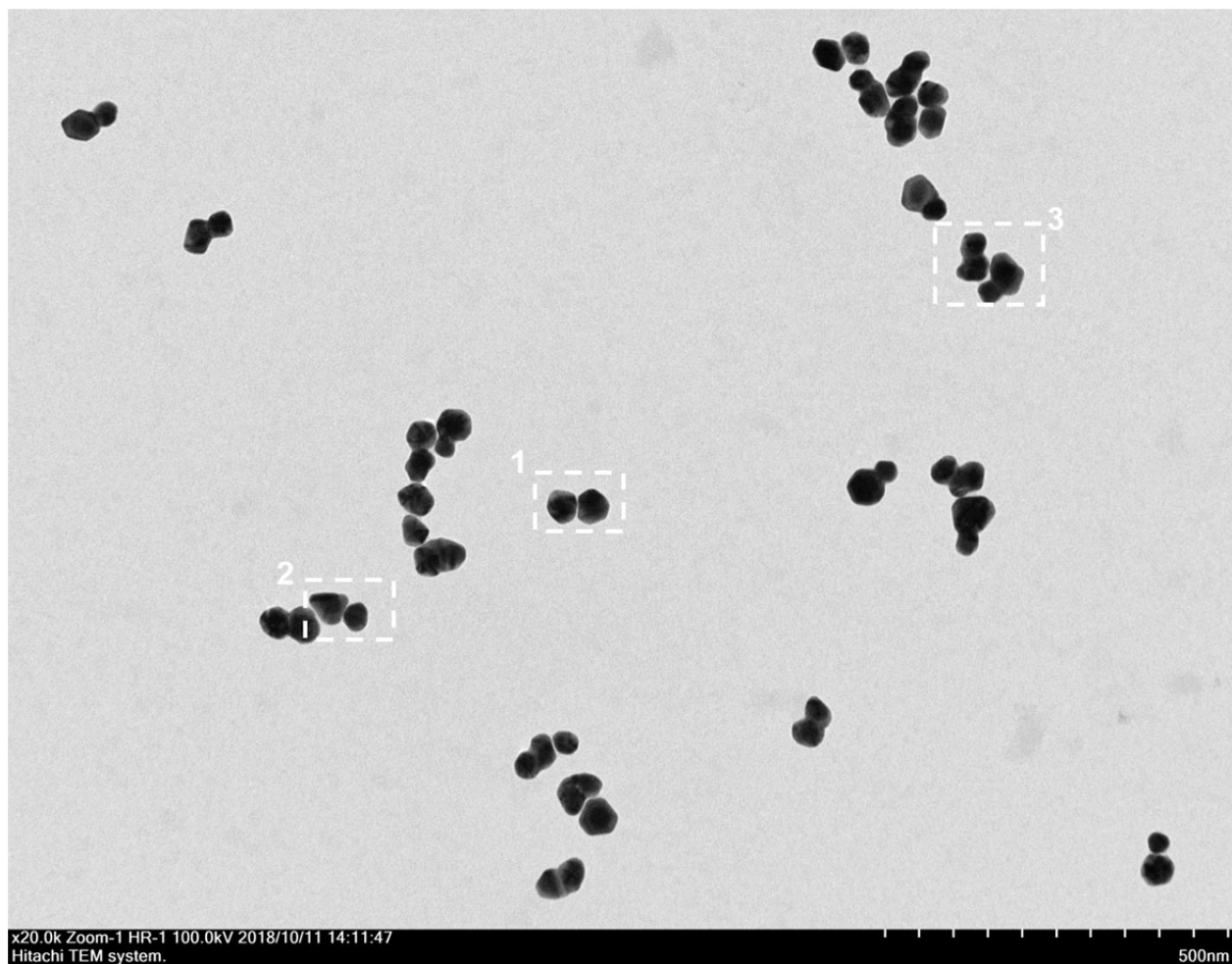
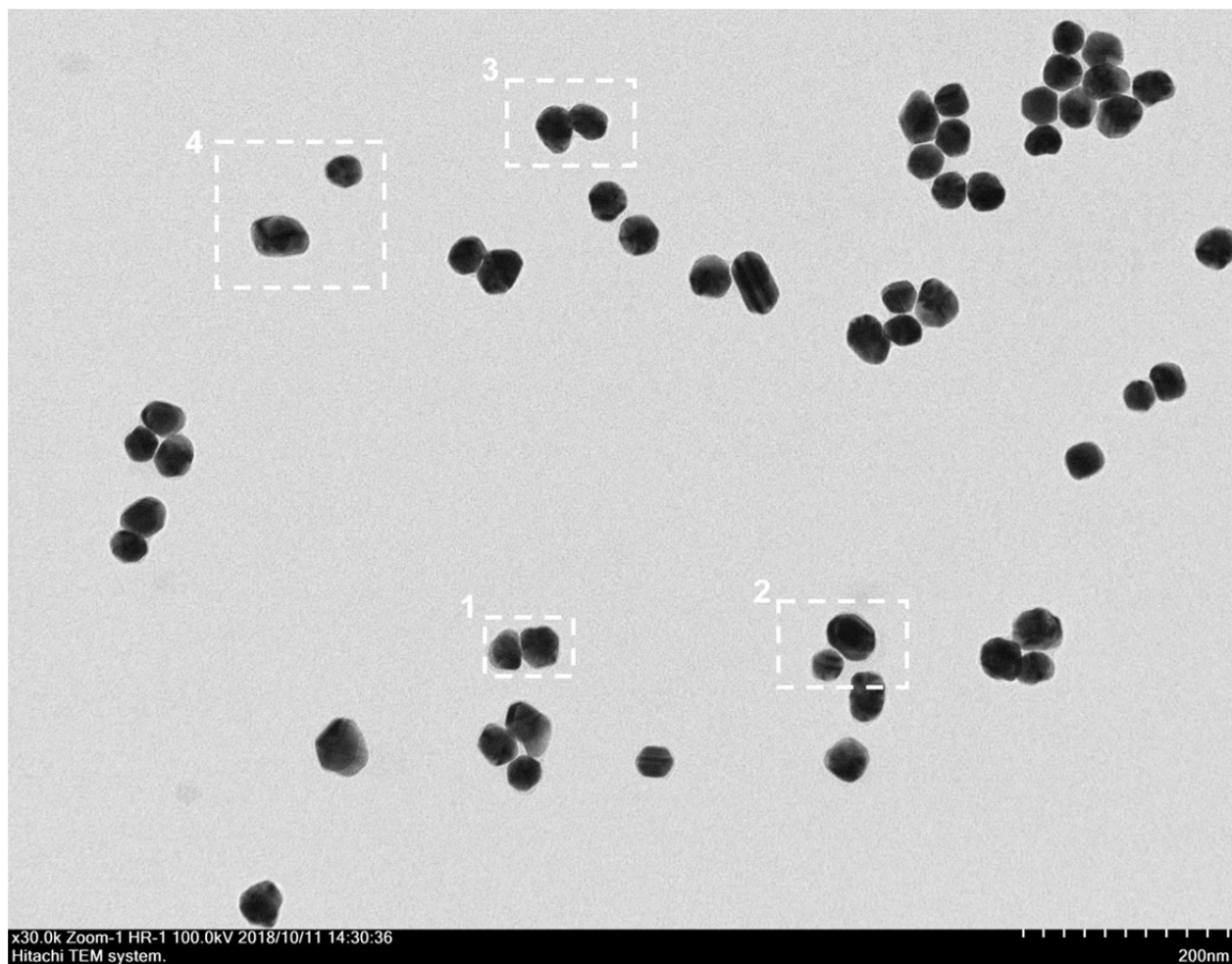


**Figure S5.** Extinction spectral characterizations revealing the critical role of reaction temperature in the formation of a silver conductive junction inside the nanogap of a strongly coupled gold nanodimer. Silver reductions by (a) L-ascorbic acid (L-AA) at 25°C and (b) sodium citrate (SC) at 85°C resulted in plasmon peaks around 400 nm (characteristic of silver nanophases) and weak, broadened CTP peaks around 650-700 nm (related to silver junctions) due to an over-deposition of silver outside of the nanogaps. In contrast, the silver deposition with SC as a reductant in a 125°C oil bath produced a very sharp CTP peak at 650 nm with unresolvable plasmon signal for the silver phase, indicating a highly preferential silver deposition in the nanogap region. Dashed profiles show the extinction spectra of the AIS-assembled gold nanodimer with a subnm interparticle gap, featuring a BDP resonance at the long wavelength side of the spectra. CTP positions are marked with triangle symbols. Please see the following TEM images showing the typical sample morphologies achieved in the 25°C and 85°C reactions.



**FigureS6.** TEM image showing typical Ag-deposited dimers at 25°C with L-AA as the reducing agent. A large portion of the structures were unsuccessful, mainly including (1) gap-retained dimers, (2) asymmetrically deposited dimers, and (3) CTP dimers with very thick Ag layer around the individual particles (not gap-preferred) (note that not all of them were marked). *This result forms a sharp contrast to Figure 3 where the reaction was conducted in a 125 °C oil bath with citrate as the reductant.*



**FigureS7.** TEM image showing typical Ag-deposited dimers at 85°C with SC as the reducing agent. A large portion of the structures were unsuccessful, mainly including (1) gap-retained dimers, (2) asymmetrically deposited dimers, (3) CTP dimers with very thick Ag layers around the individual particles (not gap-preferred), and (4) dissociated dimer assemblies (note that not all of them were marked). *This result forms a sharp contrast to Figure 3 where the reaction was conducted in a 125 °C oil bath with citrate as the reductant.*

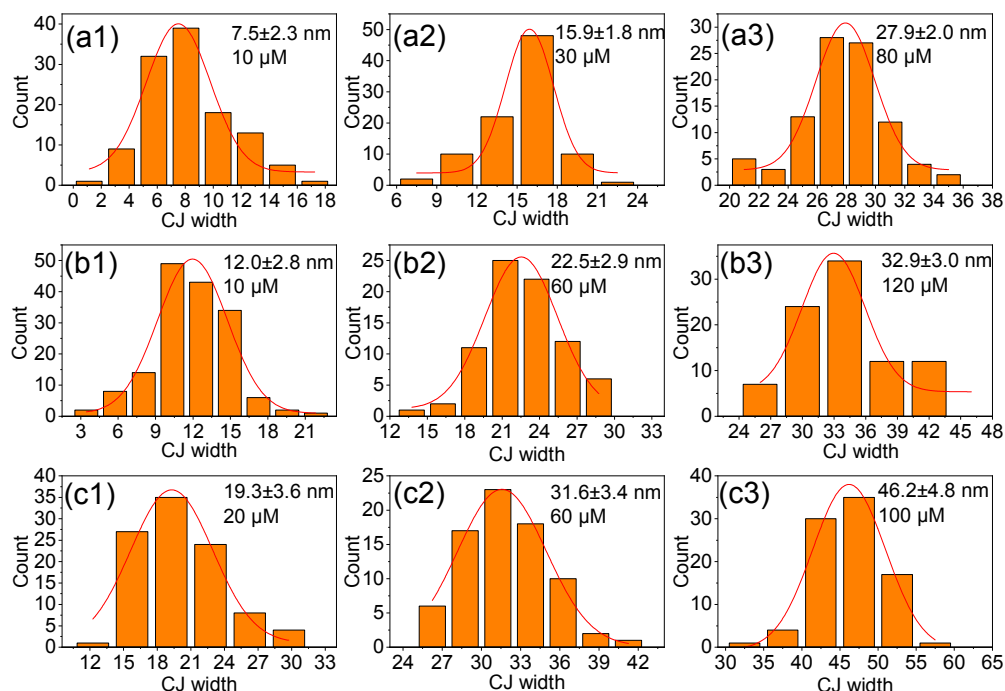


**Figure S8.** Statistical charts showing as-measured CJ widths for g-dimers made of different AuNPs (a-c corresponding to 23, 30, and 43 nm AuNPs, respectively; 1-3 correspond to different  $\text{HAuCl}_4$  concentrations as marked on each panel). Multiple TEM images of the samples were used for the analyses.

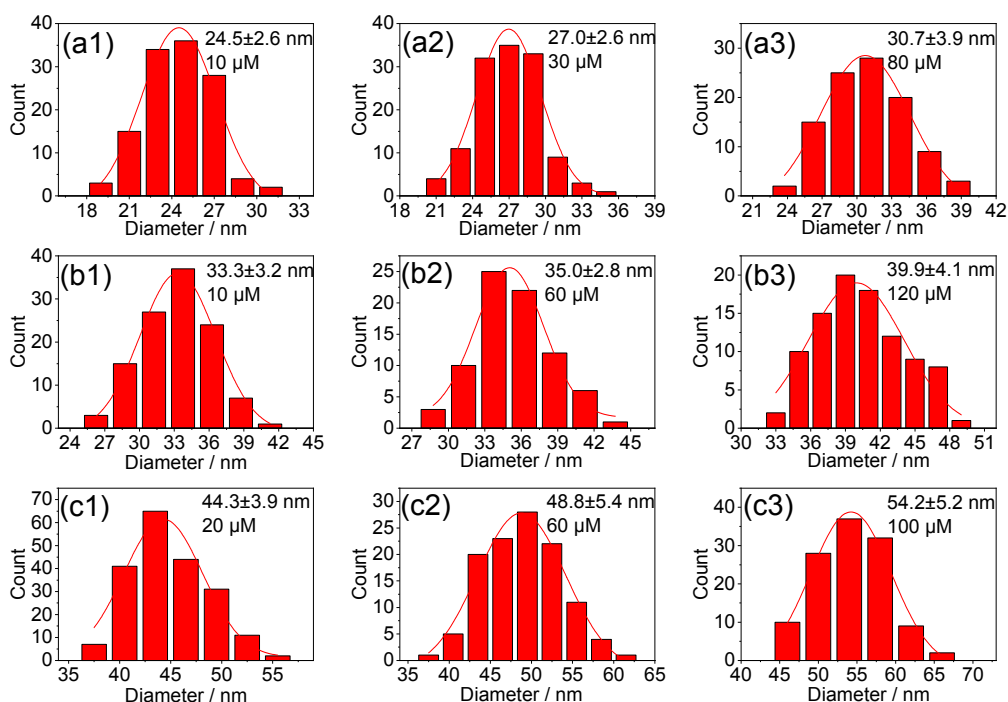


**Figure S9.** Statistical charts showing the diameters of the gold-deposited AuNPs in as-formed g-dimers. Panels a-c correspond to 23, 30, and 43 nm diameters of original AuNPs. 1-3 correspond to different  $\text{HAuCl}_4$  concentrations as marked on each panel. Multiple TEM images of the samples were used for the analyses.

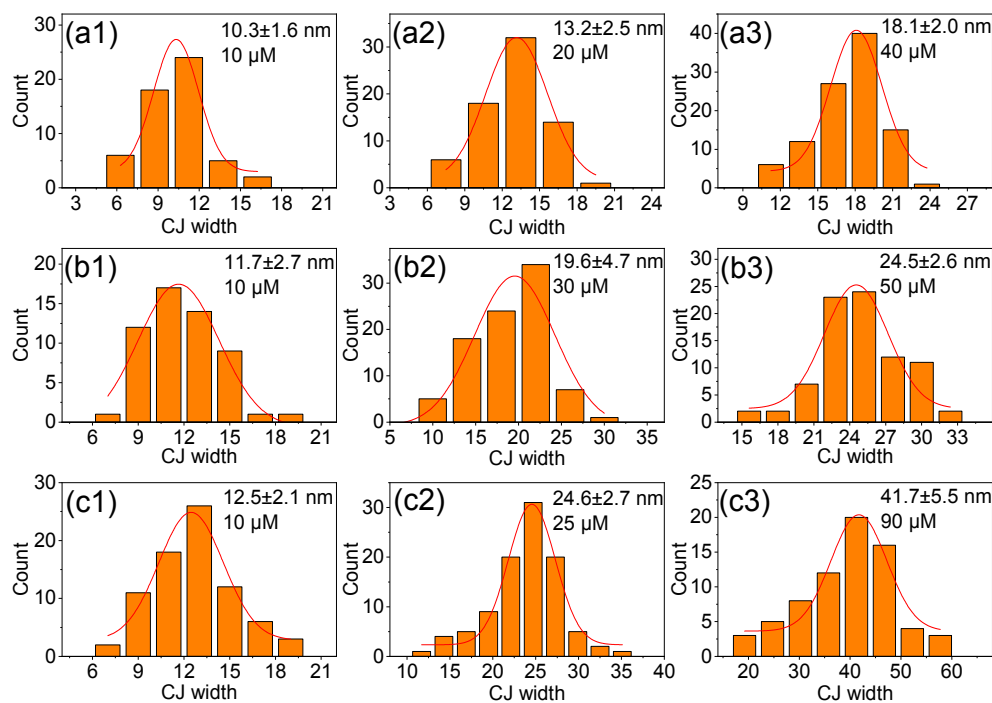


**Figure S10.** Statistical charts showing as-measured CJ widths for s-dimers made of different AuNPs (a-c corresponding to 23, 30, and 43 nm AuNPs, respectively; 1-3 correspond to different AgNO<sub>3</sub> concentrations as marked on each panel). Multiple TEM images of the samples were used for the analyses.

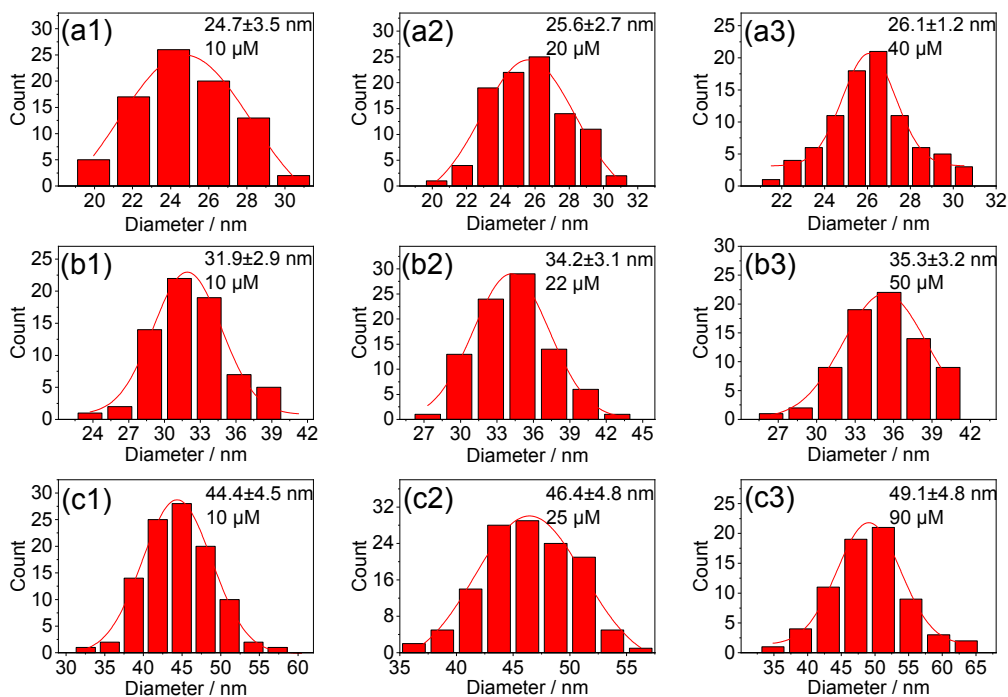


**Figure S11.** Statistical charts showing the diameters of the silver-deposited AuNPs in as-formed s-dimers. Panels a-c correspond to 23, 30, and 43 nm diameters of original AuNPs. 1-3 correspond to different AgNO<sub>3</sub> concentrations as marked on each panel. Multiple TEM images of the samples were used for the analyses.

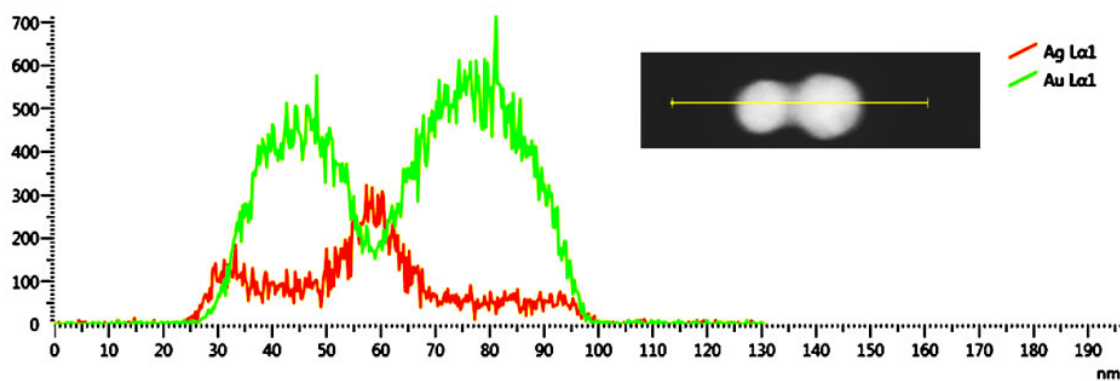


**Figure S12.** EDX analysis showing the Au and Ag element profiles along the dimer axis of a 30 nm s-dimer, indicating an enriched distribution of Ag in the gap region.

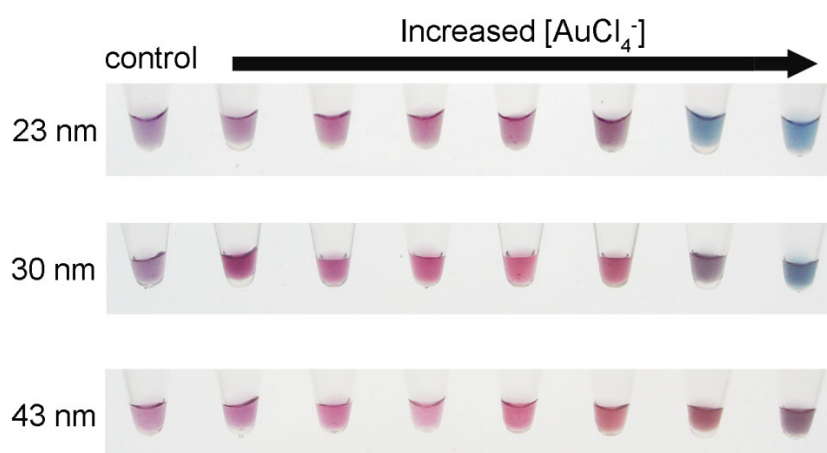


**Figure S13.** Photographs of as-formed g-dimers after reacting with different amounts of  $\text{HAuCl}_4$ . The control samples were original  $\text{Ag}^+$ -soldered dimers. These pictures show a clear color transition and a good water solubility of the products.

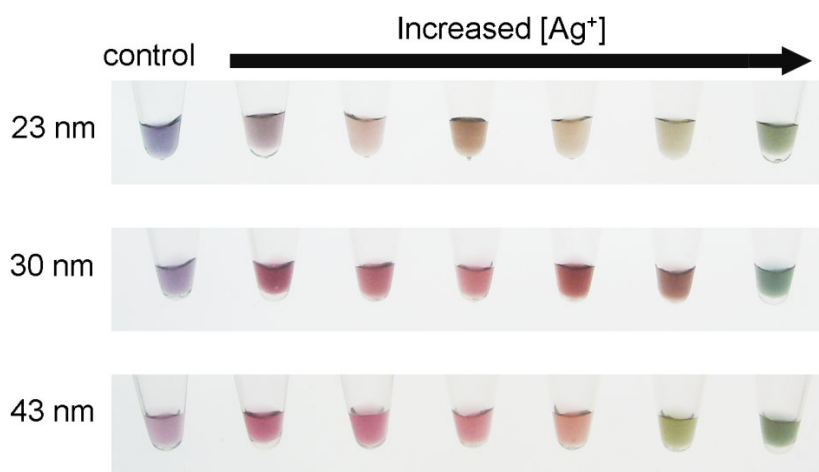


**Figure S14.** Photographs of as-formed s-dimers after reacting with different amounts of  $\text{AgNO}_3$ . The control samples were original  $\text{Ag}^+$ -soldered dimers. These pictures show a clear color transition and a good water solubility of the products.

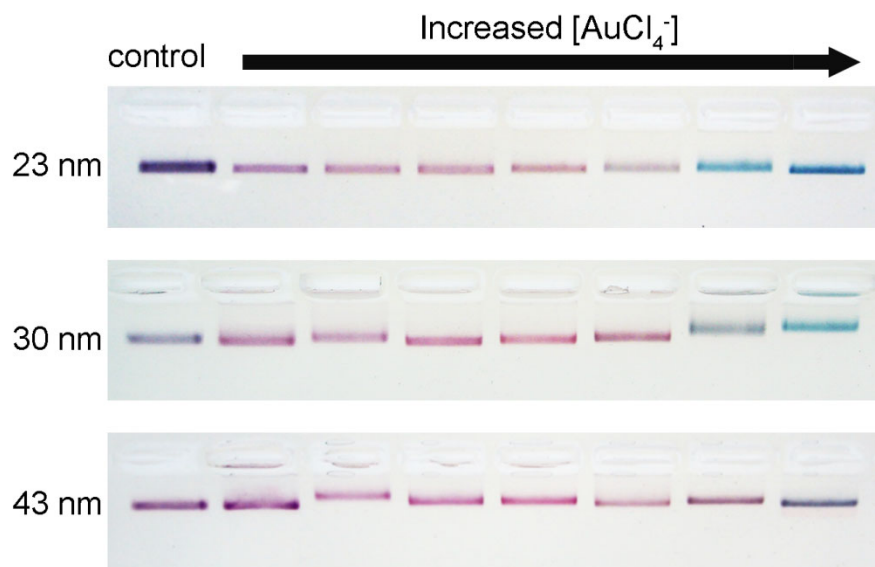


**Figure S15.** Agarose gel electropherograms of as-formed g-dimers after reacting with different amounts of  $\text{HAuCl}_4$ . The control samples were original  $\text{Ag}^+$ -soldered dimers. These data show a good purity and colloidal stability of the samples.

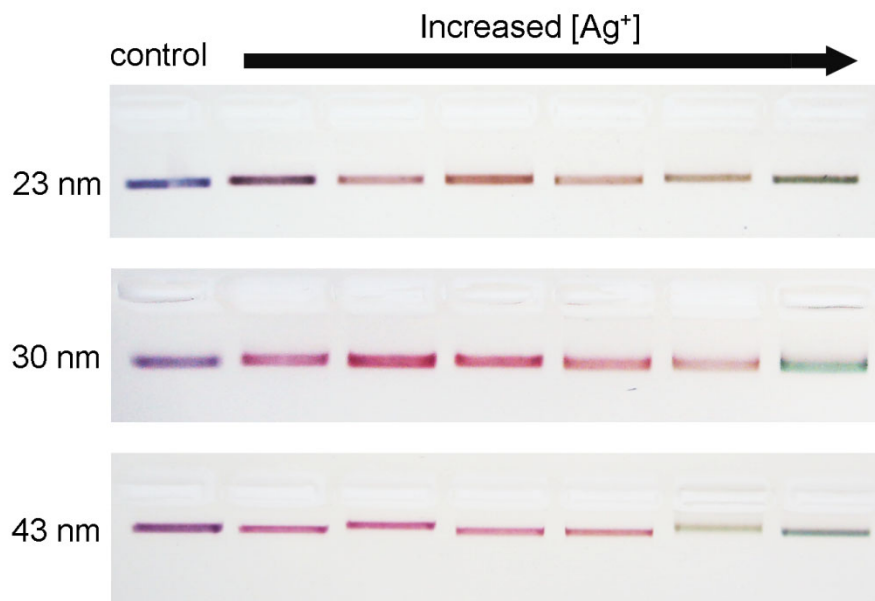


**Figure S16.** Agarose gel electropherograms of as-formed s-dimers after reacting with different amounts of  $\text{AgNO}_3$ . The control samples were original  $\text{Ag}^+$ -soldered dimers. These data show a good purity and colloidal stability of the samples.

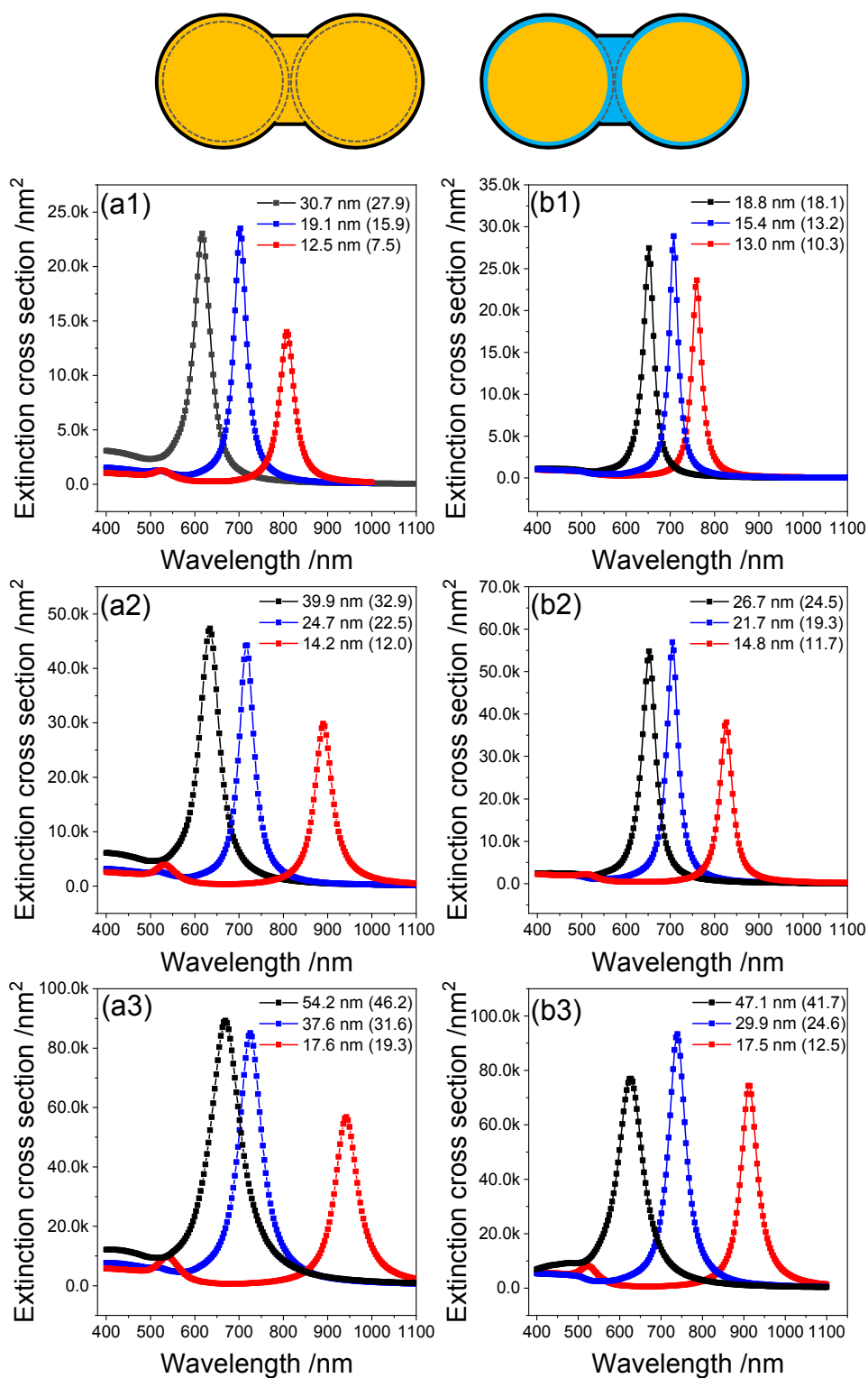


**Figure S17.** BEM calculated theoretical CTP profiles of different g-dimers (a) and s-dimers (b) based on two simplified models shown above. Light polarizations were along the dimer axes. Different CJ widths were adopted during the calculations to fit experimentally observed CTP positions (see Figure 4). The values in brackets are measured CJ widths based on TEM data, which show a good consistency with simulated ones.

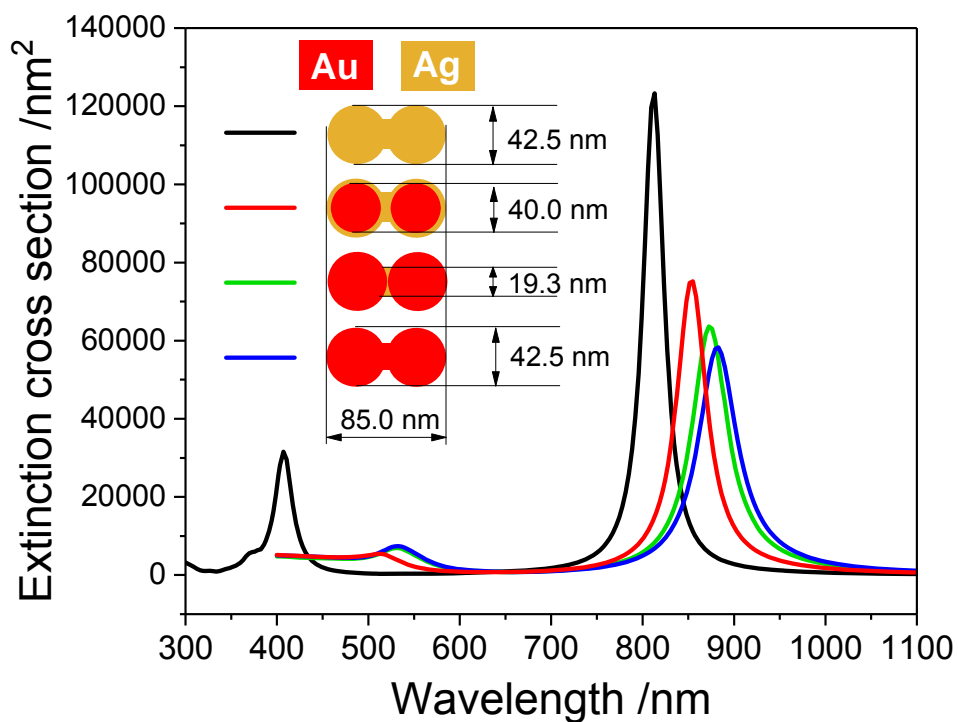


**Figure S18.** BEM calculated theoretical extinction profiles of different CTP dimers. Light polarizations were along the dimer axes. From the bottom up in the schematic drawings are: a 40 nm g-dimer bearing a 1.25 nm thick gold coating and a 19.3 nm wide Au CJ (blue curve), a 42.5 nm AuNP dimer connected by a 19.3 nm thick Ag CJ (green curve), a 40 nm s-dimer bearing a 1.25 nm thick Ag coating and a 19.3 nm wide Ag CJ (red curve), and a 42.5 nm AgNP dimer connected by a 19.3 nm wide Ag CJ (black curve).

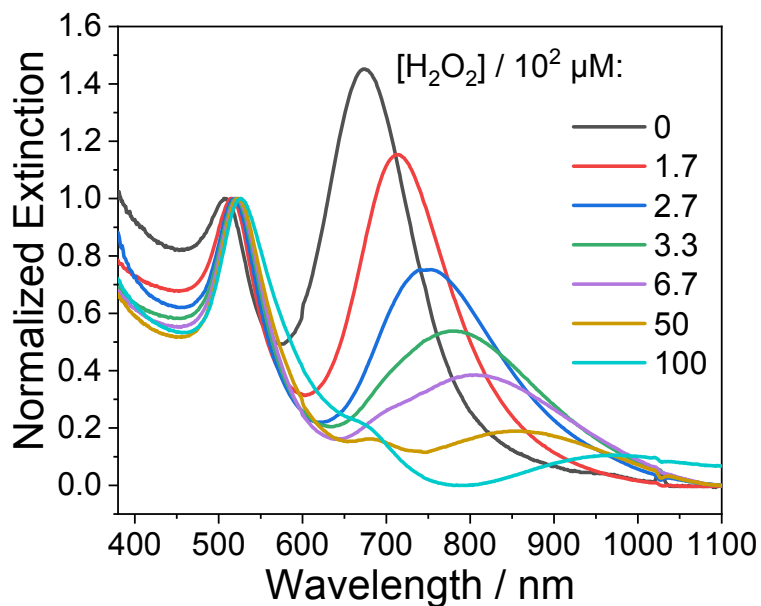


**Figure S19.** Normalized extinction spectra of s-dimers prepared from 40 nm AuNP dimers after an etching by different concentrations of  $\text{H}_2\text{O}_2$ .

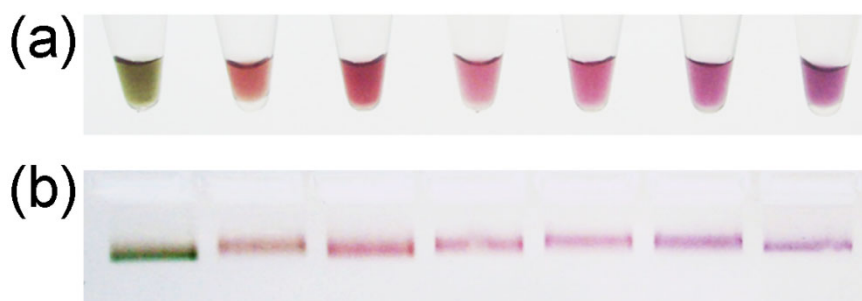


**Figure S20.** (a) Photographs of  $\text{H}_2\text{O}_2$ -etched s-dimers synthesized from 40 nm AuNP dimers. (b) Agarose gel electrophoretic data showing a good purity and colloidal stability the  $\text{H}_2\text{O}_2$ -etched s-dimers shown in (a). The samples from left to right correspond to increased  $\text{H}_2\text{O}_2$  concentrations.

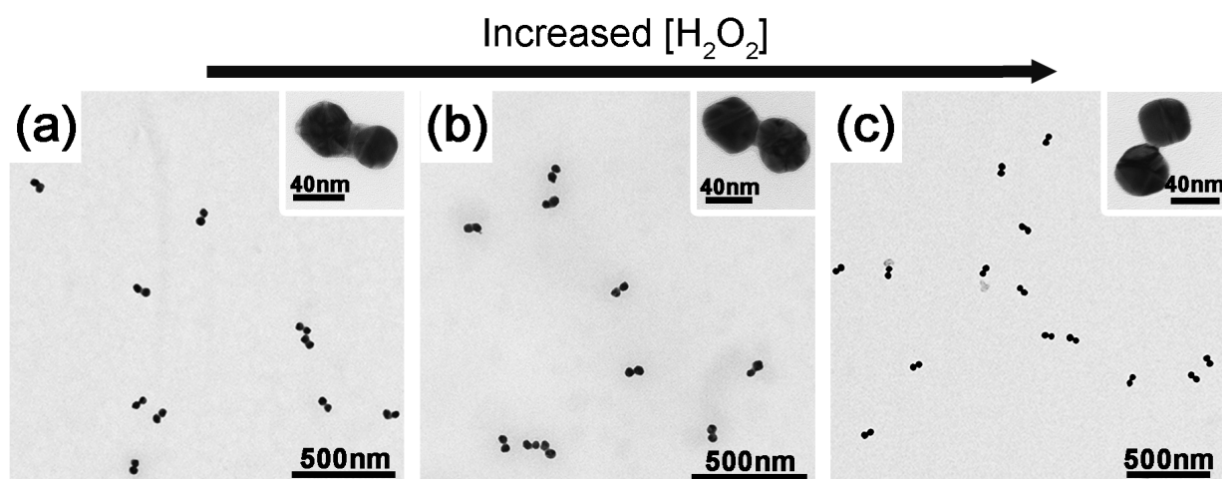


**Figure S21.** TEM images of s-dimers prepared 40 nm AuNP dimers after an etching by different concentrations of  $\text{H}_2\text{O}_2$ .

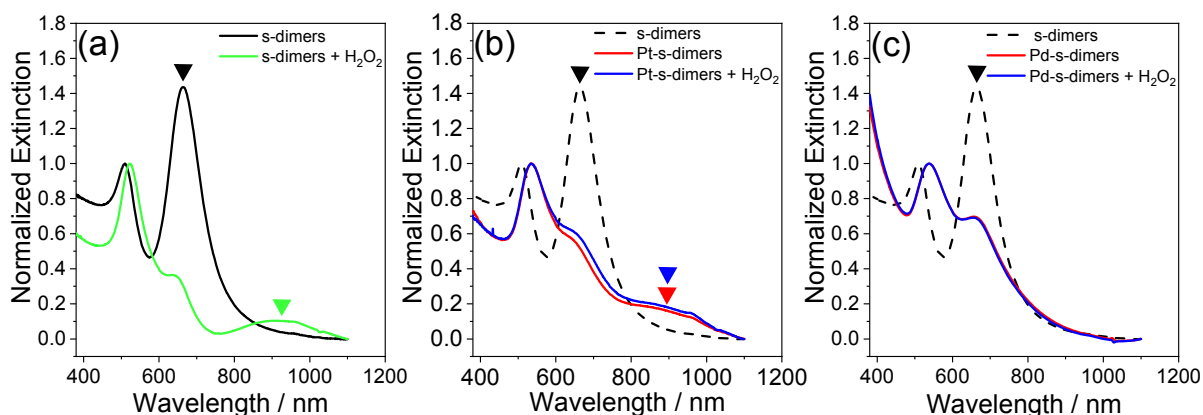


**Figure S22.** UV-visible extinction spectra of 30 nm s-dimers (a), Pt-s-dimers (b), and Pd-s-dimers (c) before and after a silver etching by  $\text{H}_2\text{O}_2$ . The negligible spectral changes for the Pt-s-dimers and Pd-s-dimers after the  $\text{H}_2\text{O}_2$  etching indicate minimal silver residuals after the Pt and Pd displacements. CTP positions are marked with triangle symbols.

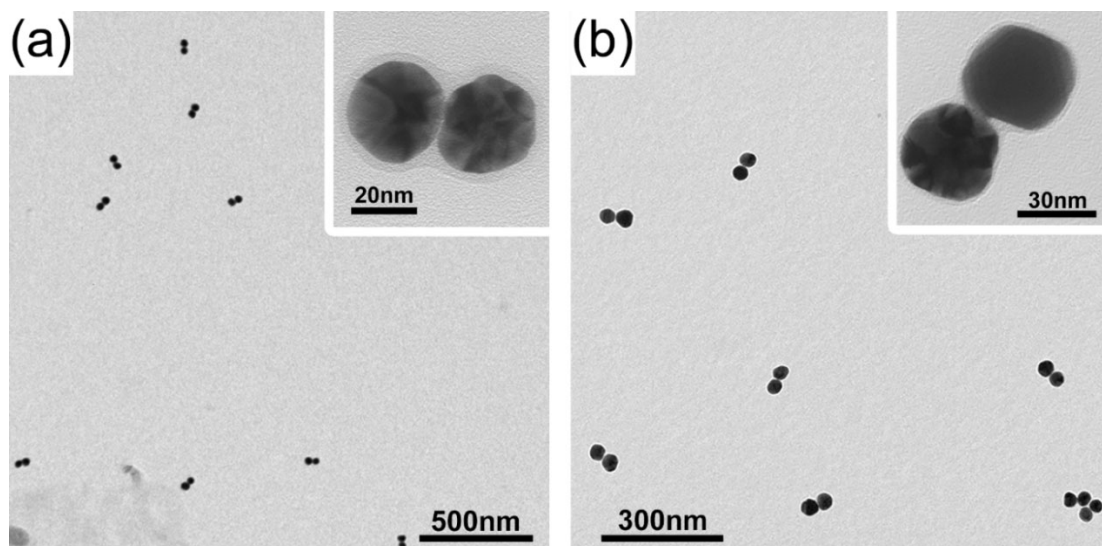


**Figure S23.** Pt-s-dimers (a) and Pd-s-dimers prepared by Galvanic displacements of s-dimers with minimum Ag deposition.

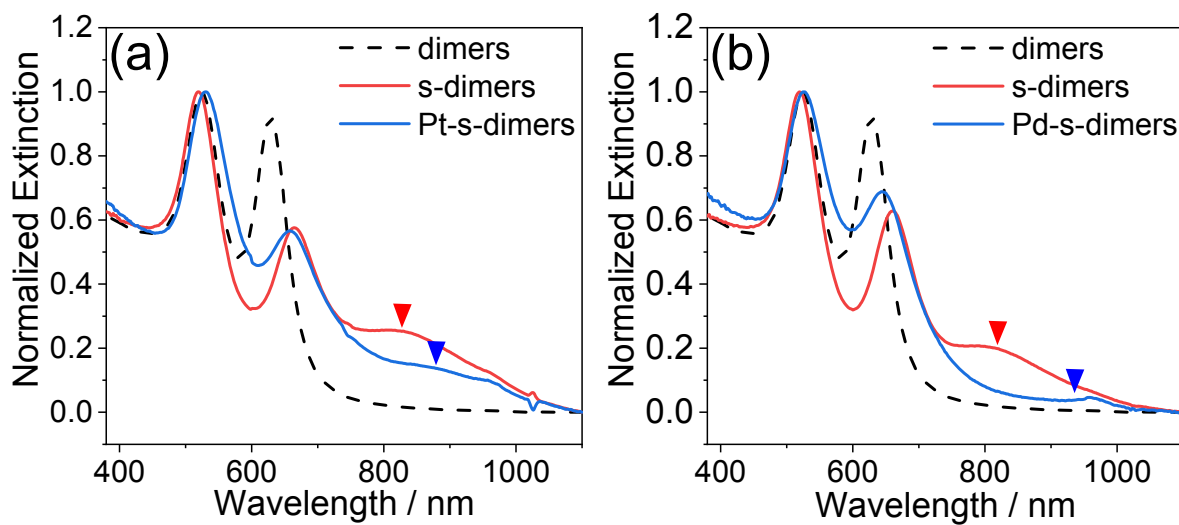


**Figure S24.** Normalized extinction spectra of Pt-s-dimers (a) and Pd-s-dimers (b) prepared by Galvanic displacements of 35 nm s-dimers with minimum Ag depositions. The weakened and redshifted CTP peaks for the Pt-s-dimers and Pd-s-dimers compared to corresponding s-dimers were a result of silver replacement.

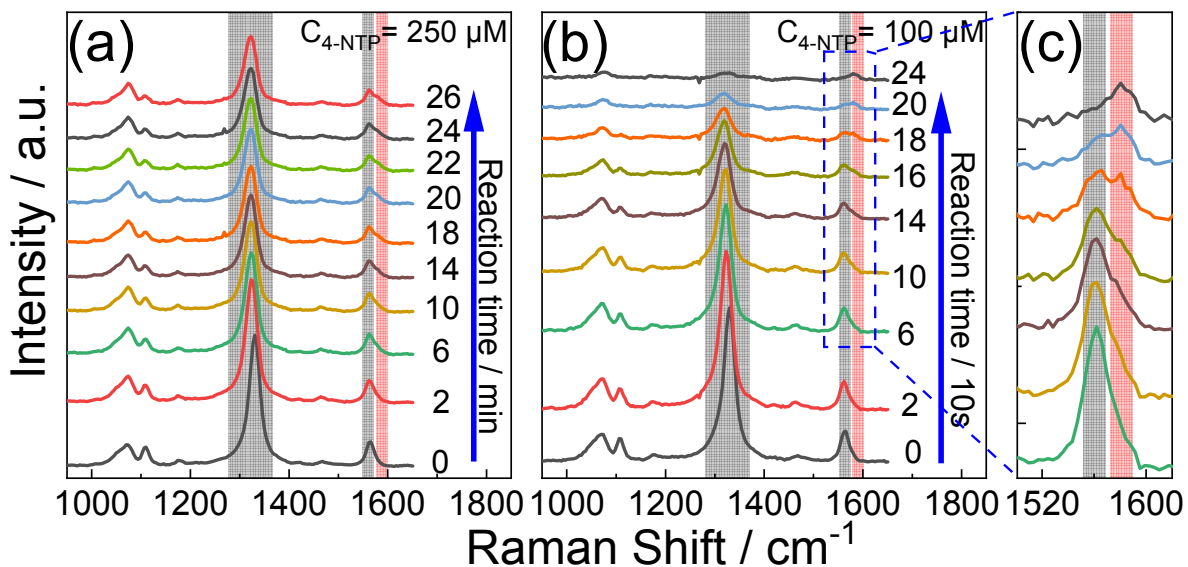


**Figure S25.** Time-course SERS spectra measured on 35 nm Pd-s-dimers showing the catalytic conversion from 4-NTP to 4-ATP after being reduced by  $\text{NaBH}_4$ . The 4-NTP-decorated Pd-s-dimers were prepared in the presence of 250  $\mu\text{M}$  (a) and 100  $\mu\text{M}$  (b) 4-NTP molecules. The catalytic conversion was obvious at a low 4-NTP coverage (panels b and c in contrasting to panel a). Panel c is a zoom-in view of the marked part in panel b.

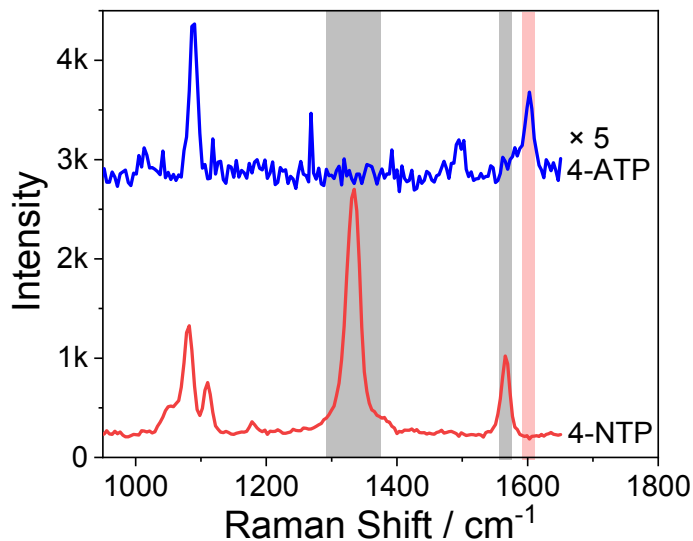


**Figure S26.** SERS spectra of chemically pure 4-NTP and 4-ATP molecules adsorbed on strongly coupled AuNP (30 nm in diameter) dimers obtained by AIS. The concentrations of 4-NTP and 4-ATP were  $10^{-5}$  M.

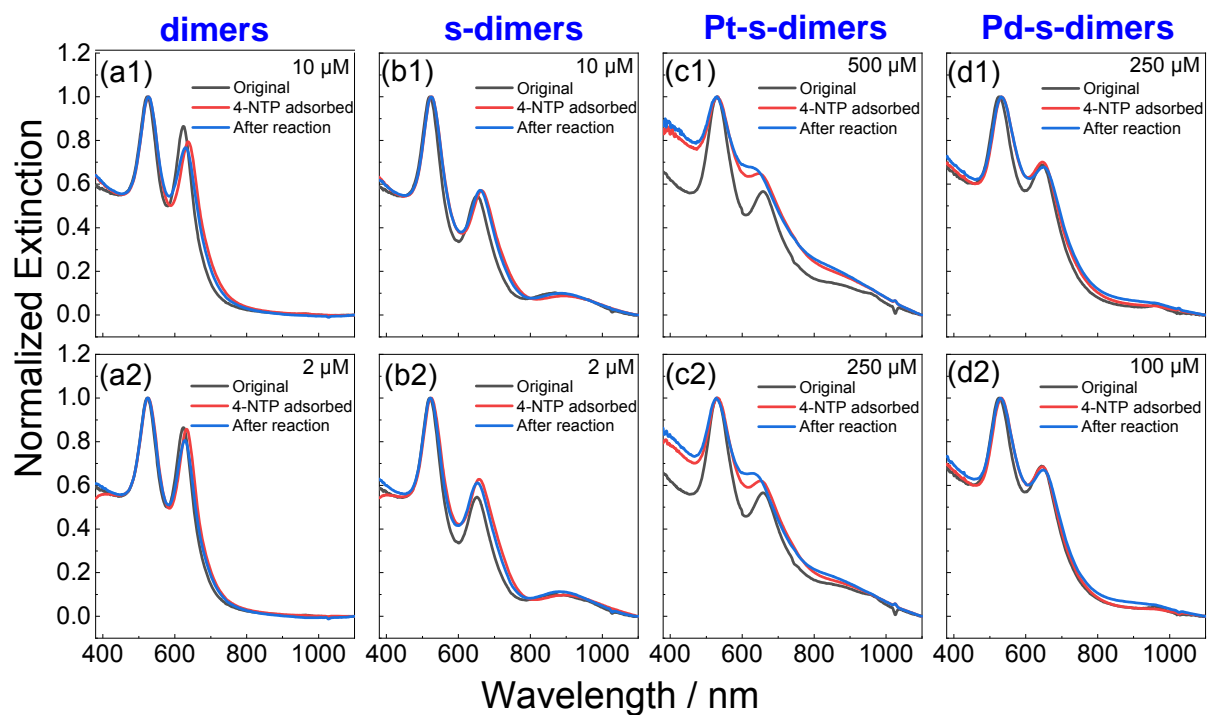


**Figure S27.** Normalized extinction spectra of AuNP dimers and different CMNFs before and after the SERS measurements. The slight changes to the BDP peaks were a result of 4-NTP and  $\text{NaBH}_4$  treatments that slightly altered the dielectric environments and gap separations of the nanofoci.

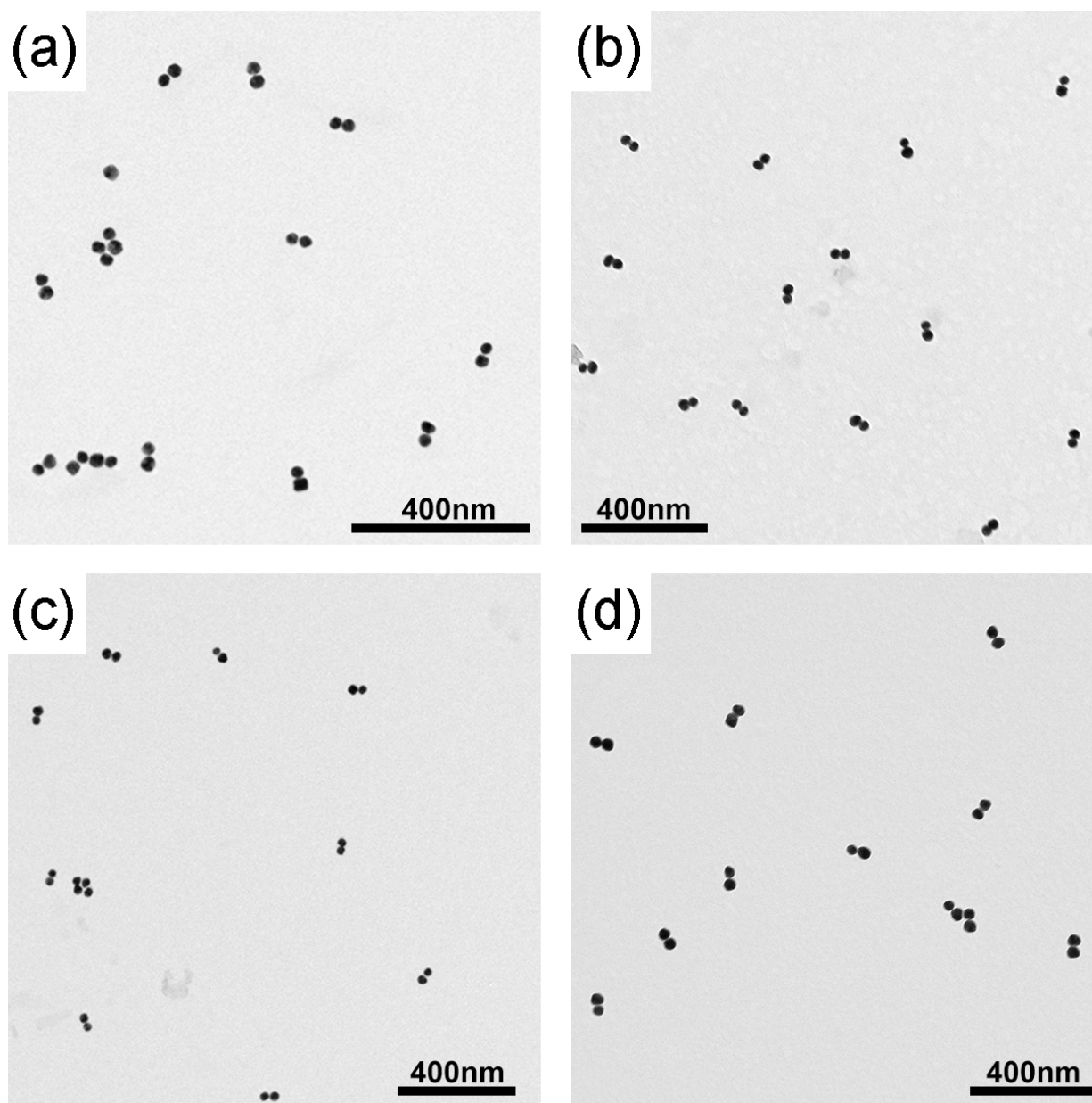


**Figure S28.** TEM images of AuNP dimers (a), s-dimers (b), Pt-s-dimers (c), and Pd-s-dimers (d) after interacting with 4-NTP and  $\text{NaBH}_4$ . These samples corresponded to the data in Figure 6.

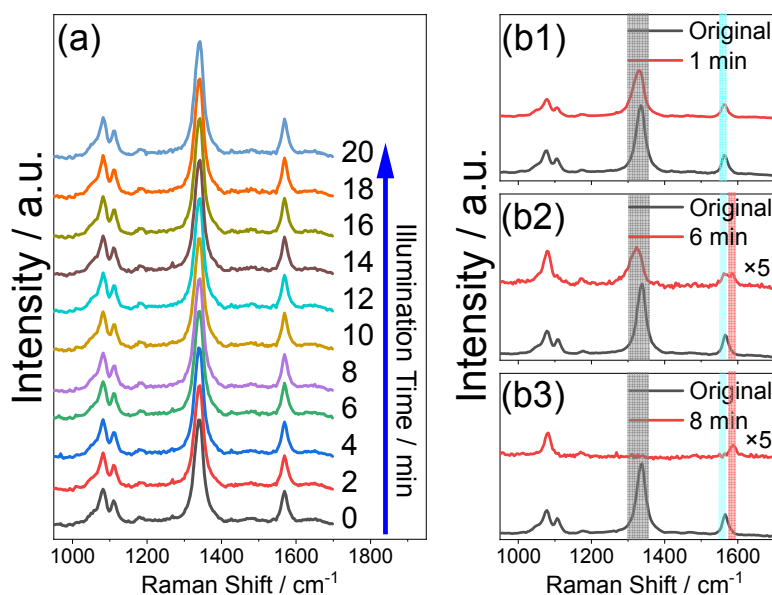


**Figure S29.** Evidences in support of the fact that only chemical catalysis was responsible for the conversion from 4-NTP to 4-ATP in the plasmonic hotspot of CMNFs. (a) Unvaried SERS signals of 4-NTP molecules adsorbed on Pt-s-dimers for different irradiation times of the 671 nm excitation laser in the absence of the chemical reductant  $\text{NaBH}_4$ . (b) Under a constant laser illumination for relatively short time of 10 s during each measurement, a prolonged incubation with  $\text{NaBH}_4$  increased the yield of 4-ATP. Shaded peaks correspond to characteristic vibrations of 4-NTP (grey and cyan) and 4-ATP (red). A complete conversion of 4-NTP into 4-ATP happened after an 8-min reaction as judged by the disappearance of 4-NTP signals. Because homogeneous solution-based samples were employed for the SERS measurements, any light-induced processes would be invisible due to a rapid diffusion of the CMNFs carrying the product molecules out of the laser focusing point. These results clearly indicate that the conversion from 4-NTP to 4-ATP was due to chemical catalysis, not related to the laser irradiation during SERS measurements.

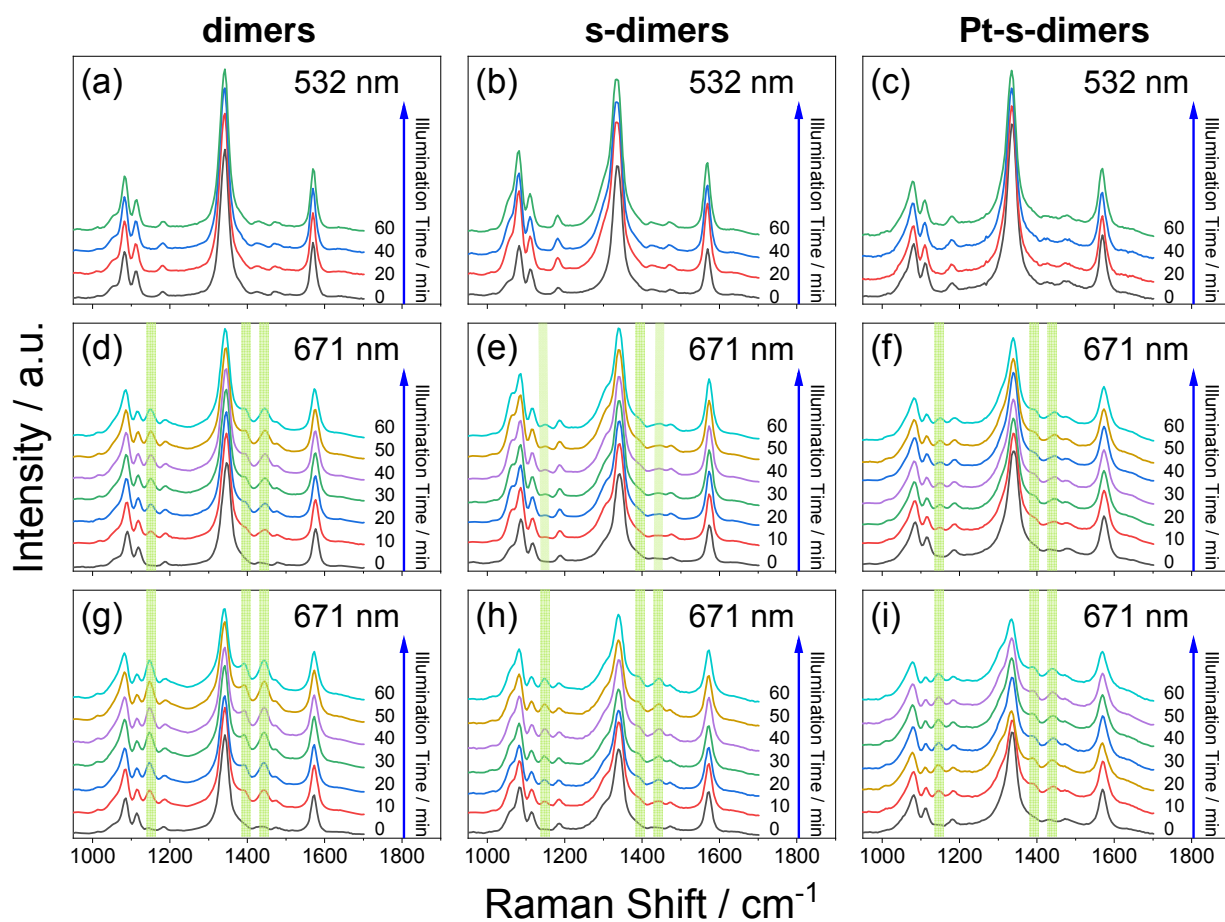


**Figure S30.** SERS spectra showing plasmon-driven dimerizations of 4-NTP into DMAB (4,4'-dimercaptoazobenzene) in the hotspots of gold nanodimers, s-dimers, and Pt-s-dimers. (a-c) Irradiation by a 532 nm laser (unmatched with the hotspot resonance) did not generate a DMAB product, as evidenced by SERS measurements with a 671 nm laser at a lowered (10%) intensity and shortened (40 s) overall illumination time to alleviate its plasmon effect. (d-i) Irradiation by a 671 nm laser at 45% (d-f) and 100% (g-i) of its full power led to clearly observable Raman signals (marked with green shadowed areas) of DMAB. The yield of DMAB was explicitly related to the laser intensity. The effectiveness of the 671 nm laser for the plasmon-driven reaction is well-understood considering the significantly red-shifted hotspot LSPR. Note that the CMNFs were deposited on a quartz substrate for the SERS measurements in order to avoid a quick diffusion of the DMAB products out of the laser focus points.

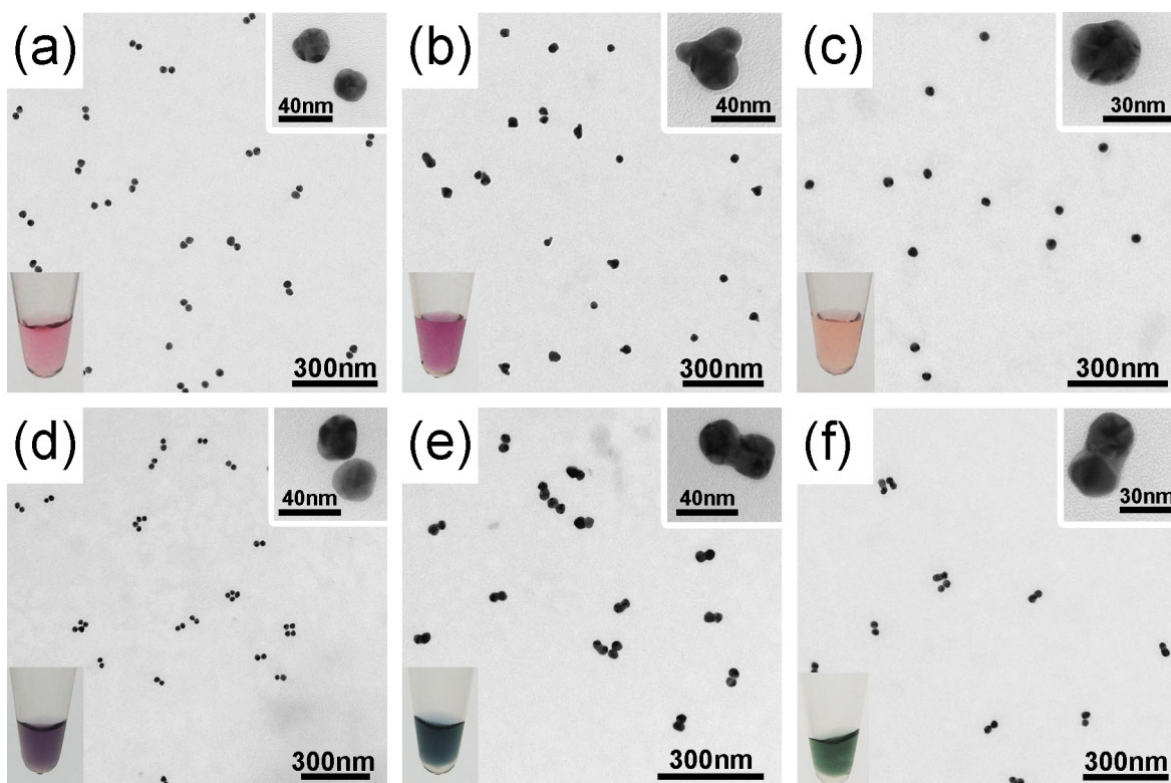


**Figure S31.** TEM images of DNA-linked 23 nm AuNP dimers before (a) and after (d) an AIS treatment, and the corresponding gold (b, e) and silver (c, f) modified nanodimers (i.e. g-dimers and s-dimers) prepared from (a) and (b) in the absence (b, c) and presence (e, f) of the AIS treatment. Insets show photographs of corresponding solutions.

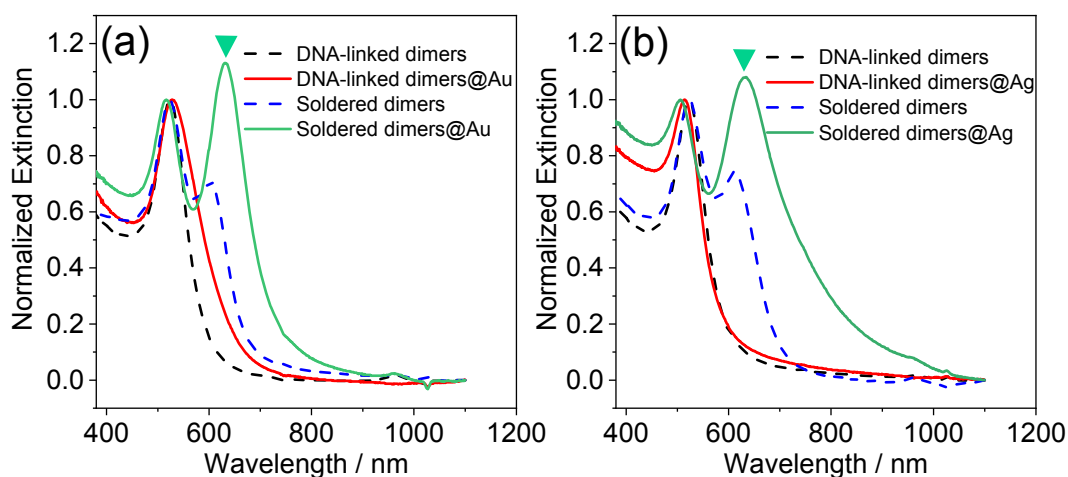


**Figure S32.** UV-visible extinction profiles of DNA-linked 23nm AuNP nanodimers, their AIS-treated structures, along with the gold (a) and silver (b) modified samples (i.e. g-dimers and s-dimers) based on the DNA-linked dimers with or without the AIS treatment. The AIS-treated dimers show a new resonance peak corresponding to the BDP mode. CTP peaks generated after a metal filling of the interparticle gaps are marked with triangle symbols.

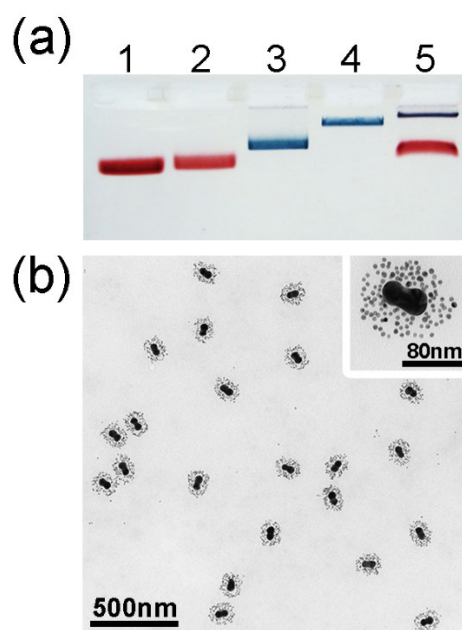


**Figure S33.** (a) Gel electrophoretic data showing a successful high density DNA functionalization of g-dimers, and their assembly with 5 nm AuNPs to form core-satellite structures. Lanes 1-5 correspond to 5 nm AuNPs (lane 1), ssDNAC mono-conjugated 5 nm AuNPs (lane 2), g-dimers (lane 3), ssDNA multi-functionalized g-dimers (lane 4), and DNA-directed core-satellite assemblies (lane 5). (b) TEM images showing the as-formed core-satellite structures with g-dimers cores (prepared from 23 nm AuNPs) and 5 nm AuNP satellites.